Published in final edited form as:
*Biochim Biophys Acta*. 2009 January 1; 1790(1): 31–39. doi:10.1016/j.bbagen.2008.09.006.

# Morelloflavone blocks injury-induced neointimal formation by inhibiting vascular smooth muscle cell migration

**Decha Pinkaew**[a,b], **Sung Gook Cho**[c], **David Y. Hui**[d], **John E. Wiktorowicz**[e], **Nongporn Hutadilok-Towatana**[b,g], **Wilawan Mahabusarakam**[e,g], **Moltira Tonganunt**[a,f], **Lewis J. Stafford**[c], **Amornrat Phongdara**[f], **Mingyao Liu**[c], and **Ken Fujise**[a,e,*]

[a]Division of Cardiology, Department of Internal Medicine, University of Texas Medical Branch, Galveston, Texas [b]Department of Biochemistry, Faculty of Science, Prince of Songkla University, Songkhla, Thailand [c]Institute of Biosciences and Technology, Texas A&M University System Health Science Center, Houston, Texas [d]Department of Pathology and Laboratory Medicine, University of Cincinnati College of Medicine, Cincinnati, Ohio [e]Department of Biochemistry and Molecular Biology, University of Texas Medical Branch, Galveston, Texas [e]Department of Chemistry, Faculty of Science, Prince of Songkla University, Songkhla, Thailand [f]Center for Genomics and Bioinformatics Research, Faculty of Science, Prince of Songkla University, Songkhla, Thailand [g]Natural Products Research Center, Prince of Songkla University, Hat-Yai, Songkhla, Thailand

## Abstract

**Background—**In-stent restenosis, or renarrowing within a coronary stent, is the most ominous complication of percutaneous coronary intervention, caused by vascular smooth muscle cell (VSMC) migration into and proliferation in the intima. Although drug-eluting stents reduce restenosis, they delay the tissue healing of the injured arteries. No promising alternative anti-restenosis treatments are currently on the horizon.

**Methods & Results—**In endothelium-denudated mouse carotid arteries, oral morelloflavone—an active ingredient of the Thai medicinal plant *Garcinia dulcis*—significantly decreased the degree of neointimal hyperplasia, without affecting neointimal cell cycle progression or apoptosis as evaluated by Ki-67 and TUNEL staining, respectively. At the cellular level, morelloflavone robustly inhibited VSMC migration as shown by both scratch wound and invasion assays. In addition, morelloflavone prevented VSMCs from forming lamellipodia, a VSMC migration apparatus. Mechanistically, the inhibition by morelloflavone of VSMC migration was through its negative regulatory effects on several migration-related kinases, including FAK, Src, ERK, and



Corresponding Author. Ken Fujise, M.D., Division of Cardiology, Department of Internal Medicine, University of Texas Medical Branch, 301 University Blvd, Suite 5.106G, Galveston, Texas, 77555. Telephone: 409-772-4885, Fax: 409-419-1777, Ken.Fujise@utmb.edu.

RhoA. Consistently with the animal data, morelloflavone did not affect VSMC cell cycle progression or induce apoptosis.

**Conclusion—**These data suggest that morelloflavone blocks injury-induced neointimal hyperplasia via the inhibition of VSMC migration, without inducing apoptosis or cell cycle arrest.

**General Significance—**We propose morelloflavone to be a viable oral agent for the prevention of restenosis, without compromising effects on the integrity and healing of the injured arteries.

### Keywords

restenosis; morelloflavone; migration; Garcinia dulcis; vascular smooth muscle cells

## Introduction

Coronary artery diseases (CAD) is the single most frequent cause of death in the U.S., accounting for more than 1 in 5 deaths and costing $133.2 billion annually [1]. Although patients with CAD can be treated either medically or surgically (coronary artery bypass grafting [CABG]), increasing numbers of patients now undergo percutaneous coronary intervention (PCI), which includes angioplasty and stent implantation. Performed in more than 900,000 patients in 2003 in the US [2], PCI, unlike CABG, does not require a thoracotomy and is much less invasive and less frequently associated with cerebrovascular complications than CABG [3]. A major disadvantage of PCI is restenosis—renarrowing of dilated or stented arteries—caused primarily by the migration and proliferation of α-actin-immunoreactive vascular smooth muscle cells (VSMCs) [4–6]. Although the use of drug-eluting stents (DES) coated with cytotoxic agents such as sirolimus [7] and paclitaxel [8] have successfully reduced restenosis, they are associated with delayed tissue healing caused by the cytotoxic and cell cycle inhibitory effects of the stent-coating drugs, necessitating the prolonged administration of anti-platelet agents [9].

*Garcinia dulcis*, a plant that belongs to the Guttiferae family, is widely distributed in Thailand, and other Southeast Asian countries [10]. Also known as Maphuut (Thailand) and Mundu (Indonesia and Malaysia), *G. dulcis* has been used in traditional medicine for centuries to treat various inflammatory conditions [11]. Several bioactive compounds, including cambogin, dulciflavan, epicathechin, lupalbigenin, mangostin, and morelloflavone, have been isolated from the plant [11, 12]. The main constituent of the leaves of *G. dulcis* (Fig. 1A) is morelloflavone (5, 7, 4′, 5″, 7″, 3‴, 4‴-heptahydroxy-[3,8″]-flavonylflavanone, CAS Registry No. 16851-21-1), a biflavonoid comprising two covalently linked flavones—apigenin and luteolin [13] (Fig. 1B). Despite the extensive medicinal use of *G. dulcis*, the biological activities of morelloflavone have not been evaluated in detail with only a few published studies [14–17].

Since several flavonoids have been reported to inhibit cell growth [18–22] and to induce apoptosis [23] in VSMCs, we hypothesized that morelloflavone—a biflavonoid—would either induce apoptosis or cell cycle arrest in VSMCs. Surprisingly, morelloflavone did neither—it blocked the migration of VSMCs without causing apoptosis or cell cycle arrest. The inhibition by morelloflavone of VSMC migration in a tissue culture system manifested

itself in decreased injury-induced neointimal hyperplasia in a mouse model of restenosis (vascular injury and neointimal formation). Based on these data, we propose that morelloflavone is a viable oral anti-restenotic agent and a potential alternative to DES-based strategies.

## Materials and Methods

### Preparation of morelloflavone

The purification of morelloflavone was performed as described previously [11] with following modifications. Dried *G. dulcis* leaves were finely powdered and extracted with acetone. Insoluble matter was removed by filtration, and the filtrate was concentrated in vacuo. A second extraction was achieved with hexane, and the hexane-insoluble fraction was subsequently extracted with dichloromethane. The greenish-yellow residue from the dichloromethane-insoluble fraction was subjected to quick-column chromatography on silica 60H and eluted with dichloromethane-acetone in a polarity gradient manner. The eluted fractions were combined on the basis of thin-layer chromatography (TLC) results. Finally, the purified compound was concentrated in vacuo, dried, and ground. TLC was used to confirm the desirable fraction for every step of extraction and purification. The purity of this compound was determined by using an HPLC system (Agilent 1100 Series, Germany), equipped with a solvent delivery pump (BinPump G1312A), an autosampler (ALS G1313A), a photodiode-array detector (DAD G1315B) and data output (LC Chemstation, Rev. A.10.02). An ODS-2 column (5 mm particle size, 4.6 × 2 50 mm i.d.; Inertsil™, Shimadzu, Japan) was used. The mobile phase, consisting of 45% (v/v) acetonitrile and 55% (v/v) of 1% acetic acid, was pumped at a flow rate of 1 ml/min, and the effluent was monitored at 289 nm. Morelloflavone in the sample was identified by comparing its spectral data with that of a standard that had been previously purified from *G. dulcis* flowers [24]. The peak analysis also revealed that the sample contained mostly morelloflavone (94.3%).

### Cell culture

Mouse VSMCs, isolated as described previously [25], were maintained in 231 media (Cascade Biologics, Portland, OR) supplemented with VSMC growth supplement (SMGS, Cascade Biologics) in a humidified incubator at 37°C with 5% $CO_2$. Cells from passages 4–9 were used in all experiments. All experiments were performed in subconfluent, unsynchronized cells growing in SMGS except for the lamellipodium formation assay.

### Cell cycle analyses

VSMCs ($1\times10^6$) were seeded onto 10-cm dishes and treated with various concentrations of morelloflavone. After 24hr incubation, the cells were fixed with 70% ethanol at 4°C overnight, treated with RNAse in PBS, stained with propidium iodide (Sigma, St. Louis, MO), and subjected to flow cytometric DNA content analysis using Epics XL (Beckman-Coulter, Miami, FL). The percentages of cells in G1, S, and G2/M phases were determined using Multi-cycle system software (Phoenix Flow System, San Diego, CA).

### 5-bromo-2-deoxyuridine (BrdU) incorporation assay

VSMCs were seeded at $2\times10^4$ cells per well in 96-well culture plates and incubated overnight. Next day, cells were found approximately 60–70% confluent. Cells were treated with various concentrations of morelloflavone (0 to 100 μM) for 2 hrs and then pulsed with BrdU at 1 μM for 8 hrs. The amount of BrdU incorporated into the cells was quantified by BrdU Cell Proliferation Assay kit (Calbiochem, San Diego, CA), according to manufacturer's instructions. Briefly, the cells were fixed and permeabilized on tissue culture plastic, and incubated with anti-BrdU monoclonal antibody. After extensive washing, bound antibodies were visualized by goat anti-mouse IgG conjugated to horseradish peroxidase and tetra-methylbenzidine substrate and quantified by spectrophotometer at 450 nm. The protein content was determined using the Bradford assay (Bio-Rad, Hercules, CA).

### 3-[4,5-Dimethylthiazol-2-yl]-2,5-diphenyltetrazolium bromide (MTT) cell survival assay

VSMCs were plated at $1\times10^4$ cells per well in 96-well culture plates and incubated overnight. The cells were treated with various concentrations of morelloflavone for 48 hrs. Then, the cells were exposed to MTT labeling reagent at 10 μg/mL for 4 hrs and solubilized in 0.01 N HCl containing 10% SDS overnight. Formed formazan was measured via spectrophotometry at 600 nm.

### DNA fragmentation assay

VSMCs were seeded at $1\times10^5$ cells per well in 24-well culture plates, treated with morelloflavone, and subjected to DNA fragmentation assay, according to the manufacturer's instructions (Cell Death Detection ELISA$^{PLUS}$, Roche). Briefly, the cells were treated with 0–100 μM of morelloflavone for 24 hrs. The $1\times10^5$ cells were lysed, cleared by centrifugation, and transferred into streptavidin-coated plates. Anti-histone antibody conjugated to biotin and anti-nucleosomal-DNA-antibody conjugated to horseradish peroxidase were added. After incubation and washing, 2,2′-azino-bis-[3-ethylbenzthiazoline-6-sulfonic acid](ABTS) substrate solution was added. The absorbance rate at 405 nm against ABTS solution was measured with the reference wavelength of 490 nm.

### Scratch wound assay

VSMCs that had been grown to confluence in 6-well culture plates were scratched with a sterile 1000-μl pipette tip and exposed to various concentrations of morelloflavone. The cells were allowed to migrate onto the plastic surface for 18 hrs and photographed. A migration index was determined based on the number of cells that migrated onto 1 $mm^2$ free plastic surface, using the Image J software (NIH).

### Invasion assay

The lower chambers of the ChemoTx® Disposable Chemotaxis System (NeuroProbe, Gaithersburg, MD) were filled with 29 μl of SMGS diluted in 231 medium at the appropriate concentrations (0–10%). A filter membrane (5 μm pore size) was positioned over the lower wells, and $1\times10^4$ VSMCs suspended in 20 μL 231 medium (without morelloflavone) were placed on the test sites within circular hydrophobic masks on the upper side of the filter

plate (n = 5 each). Cells were allowed to attach the porous membrane surface for 4 hr when solution covering cells was exchanged to 231 medium either containing 1 μM of morelloflavone or vehicle (0.1% DMSO). After additional 8-hour incubation, cells on the upper surface of the membrane—cells that had not migrated—were scraped off by Q-tips, and cells that had migrated to the lower surface were fixed and stained by hematoxylin solution and counted. Migrated cell numbers were calculated as the number of cells migrated per 8.0 [$mm^2$] test site surface area.

### Lamellipodium formation assay

The lamellipodium formation assay was performed as described previously [26]. In brief, mouse VSMCs (serum-starved for 24 hrs) were seeded onto fibronectin-coated wells of chamber slides in triplicate (CultureSlide, BD BioCoat Fibronectin) and incubated with various concentrations of morelloflavone (0, 1, and 10 μM) in the presence or absence of serum for 3 hrs at 37°C. Then, cells were fixed with 4% paraformaldehyde, permeabilized with 0.1% Triton X-100, stained with Alexa Fluor 594-Phallidin (Invitrogen-Molecular Probes) and DRAQ5 (Biostatus, Ltd, Leicestershire, UK), and viewed with the use of a Leica DM6000 confocal microscope. Four (4) fields were randomly selected per replica and the numbers of total cells and cells that exhibit lamellipodia were determined. The lamellipodium indices were calculated as the number of lamellipodia divided by the total number of cells counted.

### Western blot analysis

For the evaluation of phosphorylated focal adhesion kinase (FAK) and c-Src, Western blot analyses were performed as described previously [27]. Briefly, VSMCs were seeded on 10-cm dishes, treated with various concentrations of morelloflavone for 5 min, and harvested into RIPA buffer with protease inhibitor cocktails. Cleared cell lysates (500μg of protein) were incubated with anti-FAK or anti-c-Src antibodies at 4°C for 1 hr in a final volume of 1mL RIPA buffer, and incubated for another 1 hr with protein A/G agarose beads (Santa Cruz; SCBT sc-2003). Immunoprecipitated proteins were eluted into SDS-loading buffer and subjected to 12% SDS-PAGE and immunoblotting using anti-FAK (Santa Cruz; A-17; sc-557) and anti-c-Src (Santa Cruz; SRC-2; sc-18) antibodies for total FAK and c-Src, respectively, and anti-phosphotyrosine antibody (Santa Cruz; PY-20; sc-508) for phosphorylated FAK and c-Src. Densitometric analyses were performed using Adobe Photoshop (Adobe Systems Incorporated, San Jose, CA).

To assess the phosphorlyation status of ERK, 30μg of whole cell lysates was loaded onto SDS-PAGE, and Western blot analysis was done using anti-p-ERK (Santa Cruz; E-4; sc-7383) and anti-ERK (Santa Cruz; K-23; sc-94) antibodies.

To detect active RhoA, Rac1 and Cdc42, we first generated GST-tagged RhoA binding domain of Rhotekin protein (GST-Rhotekin-RBD) and GST-tagged p21-binding domain of p21-activated kinase 1 (PAK1)(GST-PAK1-PBD). Briefly, *E. coli* BL21 cells transformed with pGEX4T-PAK1-PBD or pGEX4T-Rhotekin-RBD were grown at 37°C and expression of recombinant protein was induced by addition of 0.1 mM IPTG for 3hrs. Cells were resuspended in lysis buffer (50 mM Tris-HCl, pH 8.0, 10% glycerol, 20% sucrose, 2 mM

DTT, 1 μg/ml leupeptin, 1 μg/ml pepstatin, and 1μg/ml aprotinin), sonicated, and centrifuged at 4°C for 30min at 45,000g. The supernatant was incubated with glutathione sepharose 4B beads (GE-Amersham, Piscataway, NJ) for 1hr at 4°C, and then washed 3 times in lysis buffer. Using these GST-proteins, we then performed GTPase activation assays as described previously [28]. Briefly, cells resuspended in lysis buffer (50 mM Tris, pH8.0, 500 mM NaCl, 1% Triton X-100, 0.1% SDS, 0.5% sodium deoxycholate, 10% glycerol, 10 mM $MgCl_2$, 10 μg/ml leupeptin and aprotinin, and 1 mM phenylmethylsulfornyl fluride) were cleared; the supernatants containing approximately 500μg of protein were incubated with 5μg of recombinant GST-Rhotekin-RBD- or GST-PAK1-PBD (both conjugated to agarose beads) for 1 hr at 4°C, washed with lysis buffer, and eluted into SDS-loading buffer. Eluents, along with cleared cell lysates, were size-fractionated by SDS-PAGE, transferred to nitrocellulose membranes, and probed by anti-RhoA, anti-Rac1, and anti-Cdc42 antibodies. Immunoreactivities on the eluents represent active forms of GTPases, whereas those on the total cell lysates represent total GTPases. These experiments were performed three times with the same results.

### Mouse carotid artery injury assay

The carotid artery injury assay was performed as described previously by Kuhel and others [29]. Male apoE$^{-/-}$ mice were obtained from Jackson Laboratory (Bar Harbor, ME) and maintained on a 12-hr light/dark cycle. All animal experimentation protocols were performed under institutional guidelines of animal welfare, in accordance with NIH guidelines. Mice were fed either normal rodent chow diet (5001, LabDiet) (n=10) or normal chow diet containing 0.15% morelloflavone (w/w) (n=9). This diet corresponded to 200 mg/kg morelloflavone if a 30-gm mouse consumes 4 grams of chow. Mice were placed on these diets for 7 days before they underwent carotid artery denudation by the insertion of an epoxy resin (Epon) probe as described previously [29]. Briefly, the entire length of the left carotid artery was exposed and the distal bifurcation of the carotid artery was looped proximally and ligated distally with 7-0 suture. A transverse arteriotomy was made between the 7-0 silk sutures and the resin probe was inserted, advanced toward the aortic arch, and withdrawn 5 times. The probe was then removed, the proximal 7-0 suture was ligated, a 6-0 suture was secured, and the incision was closed with 5-0 sterile surgical gut. After surgery, mice were maintained on these diets for 14 days before they were euthanized. After blood was sampled, the arteries of these mice were perfusion-fixed with 10% buffered formalin (pH 7.0) solution at a constant pressure of 100 mmHg. The entire neck from each mouse was dissected, fixed further in 10% buffered formalin, decalcified, and then embedded in paraffin. Identical whole neck cross sections of 5 μm were made from the distal side of the neck beginning at the point of the distal 7-0 ligature. Whole neck sections were used to evaluate both the injured and the uninjured control vessels on the same section. For each mouse, the 4 levels of serial sections were taken at 500-μm intervals. These sections were stained by Verhoeff-van Gieson (VVG) staining and subjected to morphometric analyses. Images were digitized and captured using a Sony video connected to a personal computer. Measurements were performed at a magnification of 200 using a Scion Image analysis computer program (Frederick, MD). Data were obtained from the first 2 levels where endothelial denudation occurred. For each artery, the luminal area, area inside the internal

elastic lamina (IELA), and the area encircled by external elastic lamina-IELA were measured. The intimal area (IA) was calculated as the IELA minus luminal area.

For the determination of serum morelloflavone levels, animal sera were first digested by proteinase K in the presence of 0.01% SDS. Morelloflavone was then extracted into ethyl acetate and lyophilized. The quantification of morelloflavone was performed by HPLC as described in the “preparation of morelloflavone” sub-section of Materials and Methods with following modifications. The pure morelloflavone was diluted to varying concentrations (0 – 100 μM), aliquoted into multiple tubes, and lyophilized. The samples were dissolved in 200 μL of 25% acetonitrile/0.55% acetic acid of which 100 μL were injected into a Vydac C-18 reversed phase HPLC column (Grace Davison Discovery Sciences, Deerfield, IL) in an Agilent 1100 HPLC system (San Jose, CA). Morelloflavone was eluted from the column by a 25–55% acetonitrile/0.55% linear gradient with a flow rate of 1 ml/min with UV monitoring at 289 nm. The peaks were integrated and the signal to noise value was obtained from the HPLC software, using the baseline appearing after the morelloflavone peak to calculate noise. The limit of detection (LOD) is defined as the concentration of morelloflavone that yielded a signal to noise of 2:1, and was calculated at 1.06 μM, from the 20 μM standard peak (signal to noise = 37.6:1). None of samples from control animals contained morelloflavone concentrations higher than the limit of detection.

For the analyses of intimal cell proliferation, apopotosis and ERK activation, Ki-67, Terminal deoxynucleotidyl transferase (TdT)-deoxyuridine nick-end labeling (TUNEL), and p-ERK staining, respectively, were performed. Ki-67 was detected using a monoclonal rabbit antibody (Clone TEC-3, DAKO North America, Inc., Carpinteria, CA) as described previously [30, 31]. The TUNEL staining [32] was performed using a FragEL™ DNA fragmentation detection kit (Oncogene Research Products, Boston, MA) according to the manufacturer’s instructions. The Ki-67 and apoptotic indices, defined as the number of cells with DAB-positive nuclei divided by the total number of cells counted and expressed as a percentage, were then calculated. All cells within the intima were counted.

### Statistical analysis

Values are expressed as means ± SD. Comparisons of parameters between two groups were made with Student’s *t* test. When appropriate, ANOVA was performed to compare multiple groups. A value of $P < 0.05$ was considered statistically significant.

## Results

We first prepared high-purity morelloflavone, from the leaves of *G. dulcis* (Fig. 1C). To examine the effect of morelloflavone on cell cycle progression, we treated VSMCs with 0–100 μM morelloflavone and subjected them to flow cytometric analysis. Morelloflavone at concentrations up to 10 μM did not significantly affect progression of the cell cycle; however, at 100 μM, morelloflavone blocked G2/M→G1 progression (Fig. 1D). Assays of BrdU incorporation consistently showed that morelloflavone did not significantly affect DNA synthesis at concentrations up to 10 μM ($P = 0.079$; One-way ANOVA, Tukey’s pairwise comparison) (Fig. 1E), together suggesting that morelloflavone, except at high concentrations, does not affect cell cycle progression or DNA synthesis of VSMCs.

To test the effect of morelloflavone on VSMC viability, a MTT assay was performed. Morelloflavone showed no cytotoxicity at concentrations between 0 and 10 μM ($P = 0.071$; One-way ANOVA, Fig. 1F). A standard DNA fragmentation-apoptosis assay showed that morelloflavone did not induce DNA fragmentation in VSMCs (Fig. 1G). Rather, DNA fragmentation indices decreased as morelloflavone concentrations increased (*, $P = 0.032$, Fig. 1G).

To determine whether morelloflavone plays a role in the regulation of VSMC migration, we performed a scratch wound assay. VSMCs were grown to confluency and scratched; VSMCs were allowed to migrate into the scratched area in the presence of 0, 1, 10, and 100 μM morelloflavone for the next 18 hrs. As Fig. 2A shows, the migration of VSMCs was inhibited in a concentration-dependent fashion (migration indices at 0, 1, 10 and 100 μM morelloflavone = 568.7 ± 33.5, 487.6 ± 36.9, 411.3 ± 39.5, and 191.86 ± 32.8 cells/mm$^2$, respectively; ****, $P < 0.001$ by one-way ANOVA; correlation coefficient [$r$] = − 0.976). In other words, there was a highly statistically-significant, negative correlation between morelloflavone concentrations and migration indices. In addition, there was a significant reduction in migration indices between 0 and 1 μM of morelloflavone ($P < 0.05$, Tukey's pairwise comparison). Next, to evaluate the effect of morelloflavone on VSMC invasion, a modified Boyden chamber assay was performed. VSMCs suspended in medium without morelloflavone were seeded on the upper surface of the porous membrane, which was placed on medium containing various concentrations of SMGS. Cells were allowed to attach the membrane for 3 hr when the medium was changed to one containing either morelloflavone (1 μM) or vehicle (DMSO). Cells were then allowed to migrate through 5μm pores for 8hrs. While, 0 % of SMGS did not cause VSMCs to migrate in the presence or absence of morelloflavone, the increasing concentrations of SMGS were associated with more migrated cells (Fig. 2B). In this system, morelloflavone at 1μM significantly blocked VSMC migration (***, $P = 0.002$ by two-way ANOVA, Fig. 2B). These findings, together with those presented in Fig. 2A, suggest that morelloflavone is a potent inhibitor of VSMC migration and invasion.

Our next step was to determine the effect of morelloflavone on the formation of the VSMC migratory apparatus, or the lamellipodia [26, 33]. We subjected VSMCs to serum starvation for 24 hrs and then seeded them onto fibronectin-coated wells of chamber slides. We incubated these cells in the presence and absence of sera with various concentrations (0, 1, and 10 μM) of morelloflavone. After a 3-hr incubation, cells were stained with Alexa Fluor 568-Phalloidin and examined with the use of a confocal microscope. In the absence of serum, morelloflavone at any concentration did not change the morphology of VSMCs (Fig. 2C, top panel, Serum [−] at 0, 1, and 10 μM; bottom panel, columns 1, 3 and 5). In the absence of morelloflavone, the number of lamellipodia significantly increased upon serum stimulation (Fig. 2C, top panel, Serum [−] to [+] at morelloflavone 0 μM, Fig. 2C, bottom panel, columns 1 and 2; serum [−] vs. [+] = 0.105 ± 0.006 vs. 0.05 ± 0.01, $P < 0.005$). In this system, morelloflavone significantly decreased lamellipodium indices in a concentration-dependent fashion (Fig. 2C, top panel, Serum [+] at 0, 1, and 10 μM; bottom panel, columns 2, 4, and 6 = 0, 1, and 10μM morelloflavone = 0.105 ± 0.006, 0.05 ± 0.001, 0.033 ± 0.006; ****, $P < 0.001$ by One-way ANOVA; correlation coefficient [$r$] = − 0.992).

To evaluate the pathways involved in morelloflavone-induced inhibition of VSMC migration, we studied the effect of morelloflavone on migration-related pathways. We first assessed the phosphorylation status of focal adhesion kinase (FAK) [34] and c-Src [35] by isolating these proteins by immunoprecipitation and then performing Western blot analyses on the precipitated proteins using anti-FAK, anti-c-Src, and anti-phosphotyrosine antibodies. Morelloflavone inhibited the phosphorylation of FAK and c-Src (Fig. 3A). Then, we performed a Western blot analysis using anti-ERK and anti-phosphorylated ERK antibodies on lysates from VSMCs treated with various concentrations (0–10 μM) of morelloflavone. Morelloflavone substantially inhibited the phosphorylation of ERK, a critical migration-related kinase [36] (Fig. 3B). Finally, we evaluated the effects of morelloflavone on the activation status of small GTPases involved in the regulation of cell migration [37]—RhoA, Rac1, and Cdc42. Here, we found that morelloflavone blocked the activation of RhoA at low concentrations (0.1 & 1 μM), that it blocked the activation of Cdc42 at higher concentration (10 μM), and that it had no significant effects on Rac1 (Fig. 3C). In summary, morelloflavone blocks the activation of FAK, c-Src, ERK, and RhoA (and Cdc42 at a higher concentration)—key migration-related kinases—explaining why morelloflavone can exert such a powerful inhibitory effect on migration as seen in Figs. 2A–C.

To assess whether morelloflavone's inhibitory effects on VSMC migration in vitro could reduce injury-induced neointimal formation in a whole animal, we placed apoE$^{-/-}$ mice on normal chow (n = 10) or chow containing morelloflavone (0.15% w/w, n = 9) for 1 week and induced endothelial denudation by the insertion of an epoxy resin (Epon) probe as described previously [29]. Mice were maintained on the same diets for 2 weeks before they were euthanized, and the right (uninjured) and left (injured) carotid arteries were removed. No significant differences in body weight were seen before injury (control vs. morelloflavone; 23.8 ± 2.0 vs. 24.0 ± 2.0 g, respectively, *NS*) or at the time of sacrifice (control vs. morelloflavone; 23.0 ± 1.0 vs. 23.3 ± 1.5 g, respectively, *NS*). Morelloflavone-treated mice had significantly less neointimal formation in injured carotid arteries than did control mice (Table and Fig. 4A, control vs. morelloflavone; 21769.7 ± 7862.7 μm$^2$ vs. 7862.7 ± 4047 μm$^2$, respectively; $P < 0.01$). The mean serum concentration of morelloflavone of treated animals was 1.37 ± 0.78 μM, suggesting that the effective plasma concentration of morelloflavone is around 1.37 μM. TUNEL staining showed that there is no difference in TUNEL indices between control and morelloflavone groups (control vs. morelloflavone = 19.9 ± 6.1 vs. 16.0 ± 4.6, $P = 0.23$, Fig. 4B). Ki-67 staining failed to show any difference in Ki-67 indices between control and morelloflavone groups (control vs. morelloflavone = 0.19 ± 0.34 vs. 0.17 ± 0.41 %, $P = 0.91$, Fig. 4C). These data, combined with those presented in Figs. 1 & 2, suggest that morelloflavone reduced injury-induced neointimal formation by inhibiting VSMC migration from the media to the intima in apoE$^{-/-}$ mice, but not by either increasing apoptosis or inhibiting cell proliferation in the neointima. In order to evaluate whether the inhibition by morelloflavone of ERK phosphorylation in VSMCs (Fig. 3B) can also be observed at a tissue level, we performed immunostaining of p-ERK in these sections. The p-ERK signals were seen in the neointima of 3 out of 7 tissue sections (42.9%) of control animals and in the neointima of one out of 8 sections (12.5%) of morelloflavone-treated animals (Fig. 4D), suggesting that oral

morelloflavone decreases ERK activation in the neointima—a result concordant with what was observed in the tissue culture experiment (Fig. 3B).

## Discussion

Only few reports on the anti-inflammatory and antioxidative properties of the flavonoid morelloflavone are available [12, 15–17], and its effects on vascular cells or arteries have not been studied. In this report, we have characterized the biological effects of morelloflavone on VSMCs in vitro tissue culture and in vivo injured mouse arteries. We found that morelloflavone has unique biological properties; it does not affect cell cycle progression (Figs. 1D & E) or cell survival (Figs. 1F & G) at concentrations up to 10 μM, whereas it has profound effects on migration at a concentration as low as 1 μM (Figs. 2A, B, &C). The potential mechanisms of morelloflavone's negative effect on migration include the de-activation of the migration-related molecules such as FAK, c-Src, ERk, and RhoA (Figs. 3A–C). Strikingly but consistently, oral administration of morelloflavone reduced neointimal formation in injured mouse carotid arteries (Table and Fig. 4A) without affecting the degree of apoptosis or proliferation of neointimal cells (Figs. 4B and 4C). Furthermore, oral administration of morelloflavone was also associated with the lesser degree of ERK phosphorylation (Fig. 4D).

Sirolimus, also known as rapamycin, is a potent inhibitor of VSMC migration, although its mechanism of action is unknown [38]. Unlike morelloflavone, however, sirolimus profoundly inhibits cell cycle progression of VSMCs [39] by reducing the phosphorylation of retinoblastoma protein, which arrests the cell cycle at the G1/S transition [39]. In addition, sirolimus blocks the TNF-α-NFκB-pathway and facilitates VSMC apoptosis [40]. Paclitaxel, a potent anti-microtubule agent, induces tubulin polymerization and the formation of abnormally stable and nonfunctional microtubles [41], which disrupts the normal cell cycle progression in VSMCs [42, 43] and other cell types [44]. At very low concentrations (10 nM), paclitaxel arrests the cell cycle at the G2/M phase [43, 44], unlike the G1-phase arrest by sirolimus [39]. The paclitaxel-induced cell cycle arrest is often accompanied by apoptosis [45]. Thus, morelloflavone, with its peculiar absence of profound cytotoxic and cell cycle inhibitory effects, differs from both sirolimus and paclitaxel.

Morelloflavone severely inhibited the phosphorylation of ERK at 0.1 – 10 μM (Fig. 3B). ERK is implicated in both cell cycle progression [46] and migration [47]. Intriguingly, morelloflavone—at the concentrations that reduced ERK phosphorylation—decreased cell migration (Figs 2A, 2B, and 2C) but had no effects on cell cycle progression (Figs. 1D and 1E). One explanation may be that the degree of the inhibition by morelloflavone of the phosphorylation of ERK was sufficient to negatively affect cell migration but insufficient to compromise normal cell cycle progression. Further studies are called for to evaluate these possible differential effects by morelloflavone on cell migration and cell cycle progression. In addition, although morelloflavone substantively decreased the phosphorylation of FAK, c-Src, and ERK and the activity of RhoA (Figs. 3A, 3B, and 3C)—and these molecules have been implicated in cell migration, further experiments are needed in order to clearly establish the cause-effect relationship between the inhibition by morelloflavone of these molecules and the inhibition of VSMC migration by morelloflavone.

It has been shown that Cdc42, Rac1, and RhoA act in a hierarchical cascade where Cdc42 activates Rac, which in turn activates RhoA [48]. It is not clear why morelloflavone at 10 μM inhibited Cdc42 activation without affecting Rac1 activation (Fig. 3C). It is possible that in the complex RhoGTPase network [49], morelloflavone negatively regulates Cac42 and RhoA through certain guanine nucleotide exchange factors (GEFs) specific to them. Again further studies are needed to solve this puzzle.

In the current work, we focused on the biological effects of morelloflavone on VSMCs and found that morelloflavone is a potent inhibitor of VSMC migration through the de-activation of the migration-related molecules (Figs. 3A–C). However, it is possible that morelloflavone inhibits the migration of other cell types. Further investigation is called for in order to determine whether the inhibition of VSMC migration by morelloflavone is cell-type specific.

We used ApoE$^{-/-}$ mice to test the effect of morelloflavone in injury-induced neointimal proliferation (Table and Fig. 4). This is because they exhibit far more robust neointimal proliferation than do other mouse strains such as C57BL [50] and C3H [29] because ApoE blocks injury-induced neointimal proliferation via its suppression of cyclin D1 [51].

There is an important limitation in the current study—we used mice free of atherosclerotic lesions and induced neointimal proliferation in these mice using endothelial denudation. However, human coronary restenosis occurs when severely atherosclerotic arteries are over-stretched by balloons/stents inflated at high pressures. Thus, the extraporation of the current findings to the clinical usefulness must be done with great caution. Furthermore, it is possible that the metabolite(s) of morelloflavone, in addition to morelloflavone itself, contributed to the reduction of the neointimal formation in the morelloflavone-treated animals. With that said, morelloflavone or its derivatives, with further studies, may prove to be promising anti-restenotic agents. Specifically, morelloflavone could be administered orally after the implantation of bare-metal stents to prevent in-stent restenosis. The further investigation of the compound and its derivative using larger animals is appropriate and justified given the results of the current study. Centuries of its medicinal use in Thailand and others suggest that morelloflavone is well tolerated with an acceptable toxicology profile and minimal adverse effects.

## Acknowledgments

The current study was supported in part by grants from the National Institutes of Health (HL04015 and HL68024) (to KF), the Roderick Duncan MacDonald General Research Fund at St. Luke’s Episcopal Hospital (to KF), and an Established Investigator Award from the American Heart Association (to KF). Financial support from the Thailand Research Fund through the Royal Golden Jubilee Ph.D. Graduate Program (Grant No. PHD/0215/2546) to DP and NHT is also acknowledged[1].

## List of Abbreviations

**VSMC** vascular smooth muscle cell

[1]There are no conflicts of interest.

| | |
|---|---|
| **CAD** | coronary artery disease |
| **CABG** | Coronary artery bypass grafting |
| **PCI** | percutaneous coronary intervention |
| **DES** | drug-eluting stents |
| **SMGS** | smooth muscle cells growth supplement |
| **BrdU** | 5-bromo-2-deoxyuridine |
| **MTT** | 3-[4,5-Dimethylthiazol-2-yl]-2,5-diphenyltetrazolium bromide |
| **FAK** | focal adhesion kinase |
| **IELA** | internal elastic lamina |
| **IA** | intimal area |
| **TUNEL** | Terminal deoxynucleotidyl transferase (TdT)-deoxyuridine nick-end labeling |

## References


1. American Heart Association. Heart Disease and Stroke Statistics-2004 Update. American Heart Association; Dallas: 2004.
2. Braunwald's Heart Disease. 7. Elsevier, Inc; Philadelphia: 2005.
3. Newman MF, Kirchner JL, Phillips-Bute B, Gaver V, Grocott H, Jones RH, Mark DB, Reves JG, Blumenthal JA. Longitudinal assessment of neurocognitive function after coronary-artery bypass surgery. N Engl J Med. 2001; 344:395–402. [PubMed: 11172175]
4. Morimoto S, Mizuno Y, Hiramitsu S, Yamada K, Kubo N, Nomura M, Yamaguchi T, Kitazume H, Kodama K, Kurogane H, et al. Restenosis after percutaneous transluminal coronary angioplasty--a histopathological study using autopsied hearts. Jpn Circ J. 1990; 54:43–56. [PubMed: 2332932]
5. Nobuyoshi M, Kimura T, Ohishi H, Horiuchi H, Nosaka H, Hamasaki N, Yokoi H, Kim K. Restenosis after percutaneous transluminal coronary angioplasty: pathologic observations in 20 patients. J Am Coll Cardiol. 1991; 17:433–439. [PubMed: 1991900]
6. Karsch KR, Haase KK, Wehrmann M, Hassenstein S, Hanke H. Smooth muscle cell proliferation and restenosis after stand alone coronary excimer laser angioplasty. J Am Coll Cardiol. 1991; 17:991–994. [PubMed: 1999639]
7. Moses JW, Leon MB, Popma JJ, Fitzgerald PJ, Holmes DR, O'Shaughnessy C, Caputo RP, Kereiakes DJ, Williams DO, Teirstein PS, Jaeger JL, Kuntz RE. Sirolimus-eluting stents versus standard stents in patients with stenosis in a native coronary artery. N Engl J Med. 2003; 349:1315–1323. [PubMed: 14523139]
8. Park SJ, Shim WH, Ho DS, Raizner AE, Park SW, Hong MK, Lee CW, Choi D, Jang Y, Lam R, Weissman NJ, Mintz GS. A paclitaxel-eluting stent for the prevention of coronary restenosis. N Engl J Med. 2003; 348:1537–1545. [PubMed: 12700373]
9. Iakovou I, Schmidt T, Bonizzoni E, Ge L, Sangiorgi GM, Stankovic G, Airoldi F, Chieffo A, Montorfano M, Carlino M, Michev I, Corvaja N, Briguori C, Gerckens U, Grube E, Colombo A. Incidence, predictors, and outcome of thrombosis after successful implantation of drug-eluting stents. Jama. 2005; 293:2126–2130. [PubMed: 15870416]
10. Subhadrabandhu, S. FaAOotU Nations. Under-utilized tropical fruits of Thailand. RAP Publication; 2001.
11. Deachathai S, Mahabusarakam W, Phongpaichit S, Taylor WC, Zhang YJ, Yang CR. Phenolic compounds from the flowers of Garcinia dulcis. Phytochemistry. 2006; 67:464–469. [PubMed: 16325214]

12. Deachathai S, Mahabusarakam W, Phongpaichit S, Taylor WC. Phenolic compounds from the fruit of Garcinia dulcis. Phytochemistry. 2005; 66:2368–2375. [PubMed: 16111726]
13. Verbeek R, Plomp AC, van Tol EA, van Noort JM. The flavones luteolin and apigenin inhibit in vitro antigen-specific proliferation and interferon-gamma production by murine and human autoimmune T cells. Biochemical pharmacology. 2004; 68:621–629. [PubMed: 15276069]
14. Lin YM, Anderson H, Flavin MT, Pai YH, Mata-Greenwood E, Pengsuparp T, Pezzuto JM, Schinazi RF, Hughes SH, Chen FC. In vitro anti-HIV activity of biflavonoids isolated from Rhus succedanea and Garcinia multiflora. J Nat Prod. 1997; 60:884–888. [PubMed: 9322359]
15. Gil B, Sanz MJ, Terencio MC, Gunasegaran R, Paya M, Alcaraz MJ. Morelloflavone, a novel biflavonoid inhibitor of human secretory phospholipase A2 with anti-inflammatory activity. Biochemical pharmacology. 1997; 53:733–740. [PubMed: 9113093]
16. Hutadilok-Towatana N, Kongkachuay S, Mahabusarakam W. Inhibition of human lipoprotein oxidation by morelloflavone and camboginol from Garcinia dulcis. Nat Prod Res. 2007; 21:655–662. [PubMed: 17613824]
17. Sanz MJ, Ferrandiz ML, Cejudo M, Terencio MC, Gil B, Bustos G, Ubeda A, Gunasegaran R, Alcaraz MJ. Influence of a series of natural flavonoids on free radical generating systems and oxidative stress. Xenobiotica. 1994; 24:689–699. [PubMed: 7975732]
18. Han HJ, Kim TJ, Jin YR, Hong SS, Hwang JH, Hwang BY, Lee KH, Park TK, Yun YP. Cudraflavanone A, a flavonoid isolated from the root bark of Cudrania tricuspidata, inhibits vascular smooth muscle cell growth via an Akt-dependent pathway. Planta medica. 2007; 73:1163–1168. [PubMed: 17713875]
19. Huang HC, Wang HR, Hsieh LM. Antiproliferative effect of baicalein, a flavonoid from a Chinese herb, on vascular smooth muscle cell. European journal of pharmacology. 1994; 251:91–93. [PubMed: 8137874]
20. Kim TJ, Zhang YH, Kim Y, Lee CK, Lee MK, Hong JT, Yun YP. Effects of apigenin on the serum- and platelet derived growth factor-BB-induced proliferation of rat aortic vascular smooth muscle cells. Planta medica. 2002; 68:605–609. [PubMed: 12142993]
21. Kim TJ, Kim JH, Jin YR, Yun YP. The inhibitory effect and mechanism of luteolin 7-glucoside on rat aortic vascular smooth muscle cell proliferation. Archives of pharmacal research. 2006; 29:67–72. [PubMed: 16491846]
22. Kim JH, Jin YR, Park BS, Kim TJ, Kim SY, Lim Y, Hong JT, Yoo HS, Yun YP. Luteolin prevents PDGF-BB-induced proliferation of vascular smooth muscle cells by inhibition of PDGF beta-receptor phosphorylation. Biochemical pharmacology. 2005; 69:1715–1721. [PubMed: 15935146]
23. Perez-Vizcaino F, Bishop-Bailley D, Lodi F, Duarte J, Cogolludo A, Moreno L, Bosca L, Mitchell JA, Warner TD. The flavonoid quercetin induces apoptosis and inhibits JNK activation in intimal vascular smooth muscle cells. Biochemical and biophysical research communications. 2006; 346:919–925. [PubMed: 16777073]
24. Phongpaichit S, Rungjindamai N, Rukachaisirikul V, Sakayaroj J. Antimicrobial activity in cultures of endophytic fungi isolated from Garcinia species. FEMS Immunol Med Microbiol. 2006; 48:367–372. [PubMed: 17052267]
25. Ross R. The smooth muscle cell. II. Growth of smooth muscle in culture and formation of elastic fibers. J Cell Biol. 1971; 50:172–186. [PubMed: 4327464]
26. Liu D, Hou J, Hu X, Wang X, Xiao Y, Mou Y, De Leon H. Neuronal chemorepellent Slit2 inhibits vascular smooth muscle cell migration by suppressing small GTPase Rac1 activation. Circulation research. 2006; 98:480–489. [PubMed: 16439689]
27. Guo X, Stafford LJ, Bryan B, Xia C, Ma W, Wu X, Liu D, Songyang Z, Liu M. A Rac/Cdc42-specific exchange factor, GEFT, induces cell proliferation, transformation, and migration. The Journal of biological chemistry. 2003; 278:13207–13215. [PubMed: 12547822]
28. Sander EE, van Delft S, ten Klooster JP, Reid T, van der Kammen RA, Michiels F, Collard JG. Matrix-dependent Tiam1/Rac signaling in epithelial cells promotes either cell-cell adhesion or cell migration and is regulated by phosphatidylinositol 3-kinase. J Cell Biol. 1998; 143:1385–1398. [PubMed: 9832565]

29. Kuhel DG, Zhu B, Witte DP, Hui DY. Distinction in genetic determinants for injury-induced neointimal hyperplasia and diet-induced atherosclerosis in inbred mice. Arteriosclerosis, thrombosis, and vascular biology. 2002; 22:955–960.
30. Ihling C, Haendeler J, Menzel G, Hess RD, Fraedrich G, Schaefer HE, Zeiher AM. Co-expression of p53 and MDM2 in human atherosclerosis: implications for the regulation of cellularity of atherosclerotic lesions. J Pathol. 1998; 185:303–312. [PubMed: 9771485]
31. Ihling C, Menzel G, Wellens E, Monting JS, Schaefer HE, Zeiher AM. Topographical association between the cyclin-dependent kinases inhibitor P21, p53 accumulation, and cellular proliferation in human atherosclerotic tissue. Arteriosclerosis, thrombosis, and vascular biology. 1997; 17:2218–2224.
32. Surh CD, Sprent J. T-cell apoptosis detected in situ during positive and negative selection in the thymus. Nature. 1994; 372:100–103. [PubMed: 7969401]
33. Small JV, Stradal T, Vignal E, Rottner K. The lamellipodium: where motility begins. Trends Cell Biol. 2002; 12:112–120. [PubMed: 11859023]
34. Ilic D, Furuta Y, Kanazawa S, Takeda N, Sobue K, Nakatsuji N, Nomura S, Fujimoto J, Okada M, Yamamoto T. Reduced cell motility and enhanced focal adhesion contact formation in cells from FAK-deficient mice. Nature. 1995; 377:539–544. [PubMed: 7566154]
35. Klinghoffer RA, Sachsenmaier C, Cooper JA, Soriano P. Src family kinases are required for integrin but not PDGFR signal transduction. Embo J. 1999; 18:2459–2471. [PubMed: 10228160]
36. Nguyen DH, Catling AD, Webb DJ, Sankovic M, Walker LA, Somlyo AV, Weber MJ, Gonias SL. Myosin light chain kinase functions downstream of Ras/ERK to promote migration of urokinase-type plasminogen activator-stimulated cells in an integrin-selective manner. J Cell Biol. 1999; 146:149–164. [PubMed: 10402467]
37. Gerthoffer WT. Mechanisms of vascular smooth muscle cell migration. Circulation research. 2007; 100:607–621. [PubMed: 17363707]
38. Poon M, Marx SO, Gallo R, Badimon JJ, Taubman MB, Marks AR. Rapamycin inhibits vascular smooth muscle cell migration. The Journal of clinical investigation. 1996; 98:2277–2283. [PubMed: 8941644]
39. Marx SO, Jayaraman T, Go LO, Marks AR. Rapamycin-FKBP inhibits cell cycle regulators of proliferation in vascular smooth muscle cells. Circulation research. 1995; 76:412–417. [PubMed: 7532117]
40. Giordano A, Avellino R, Ferraro P, Romano S, Corcione N, Romano MF. Rapamycin antagonizes NF-kappaB nuclear translocation activated by TNF-alpha in primary vascular smooth muscle cells and enhances apoptosis. Am J Physiol Heart Circ Physiol. 2006; 290:H2459–2465. [PubMed: 16428340]
41. Schiff PB, Fant J, Horwitz SB. Promotion of microtubule assembly in vitro by taxol. Nature. 1979; 277:665–667. [PubMed: 423966]
42. Axel DI, Kunert W, Goggelmann C, Oberhoff M, Herdeg C, Kuttner A, Wild DH, Brehm BR, Riessen R, Koveker G, Karsch KR. Paclitaxel inhibits arterial smooth muscle cell proliferation and migration in vitro and in vivo using local drug delivery. Circulation. 1997; 96:636–645. [PubMed: 9244237]
43. Wiskirchen J, Schober W, Schart N, Kehlbach R, Wersebe A, Tepe G, Claussen CD, Duda SH. The effects of paclitaxel on the three phases of restenosis: smooth muscle cell proliferation, migration, and matrix formation: an in vitro study. Invest Radiol. 2004; 39:565–571. [PubMed: 15308939]
44. Liebmann J, Cook JA, Lipschultz C, Teague D, Fisher J, Mitchell JB. The influence of Cremophor EL on the cell cycle effects of paclitaxel (Taxol) in human tumor cell lines. Cancer Chemother Pharmacol. 1994; 33:331–339. [PubMed: 7904231]
45. Wang TH, Wang HS, Soong YK. Paclitaxel-induced cell death: where the cell cycle and apoptosis come together. Cancer. 2000; 88:2619–2628. [PubMed: 10861441]
46. Chambard JC, Lefloch R, Pouyssegur J, Lenormand P. ERK implication in cell cycle regulation. Biochimica et biophysica acta. 2007; 1773:1299–1310. [PubMed: 17188374]

47. Matsusaka S, Wakabayashi I. 5-Hydroxytryptamine augments migration of human aortic smooth muscle cells through activation of RhoA and ERK. Biochemical and biophysical research communications. 2005; 337:916–921. [PubMed: 16219295]

48. Hall A. Rho GTPases and the actin cytoskeleton. Science (New York, NY. 1998; 279:509–514.

49. Bar-Sagi D, Hall A. Ras and Rho GTPases: a family reunion. Cell. 2000; 103:227–238. [PubMed: 11057896]

50. Zhu B, Reardon CA, Getz GS, Hui DY. Both apolipoprotein E and immune deficiency exacerbate neointimal hyperplasia after vascular injury in mice. Arteriosclerosis, thrombosis, and vascular biology. 2002; 22:450–455.

51. Zhu B, Kuhel DG, Witte DP, Hui DY. Apolipoprotein E inhibits neointimal hyperplasia after arterial injury in mice. The American journal of pathology. 2000; 157:1839–1848. [PubMed: 11106557]

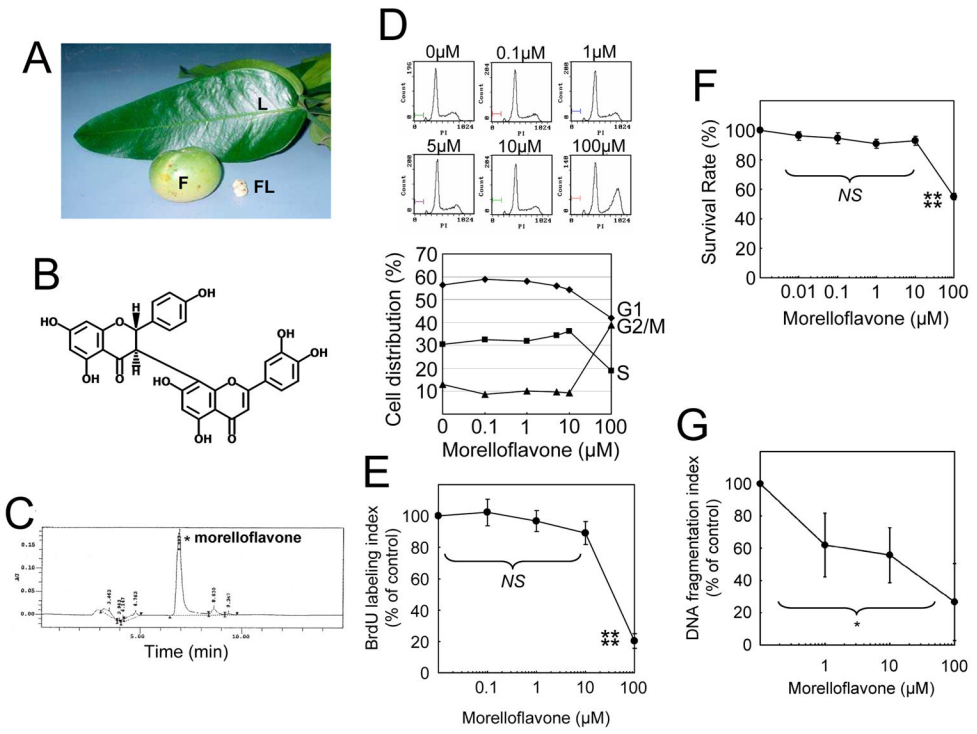


**Fig. 1. Morelloflavone does not affect cell cycle progression and causes no cytotoxicity or apoptosis in VSMCs**

***(A) Garcinia dulis.*** L, the leaves; F, fruit; FL, flower. ***(B) Structure of morelloflavone***. Morelloflavone (MW = 556), a biflavonoid, consists of two flavones covalently linked to each other. ***(C) Purification and characterization of morelloflavone.*** The current preparation of morelloflavone was purified from the leaves of *Garcinia dulis* and found to be 93.4% pure as determined by HPLC. ***(D) Flow cytometric analysis.*** Cell cycle progression was evaluated by treating VSMCs with various concentrations (0–100 μM) of morelloflavone and subjecting them to flow cytometric analyses (representative data from 3 independent experiments). ***(E) BrdU assays.*** The percentage of S-phase cells were determined by treating VSMCs with various concentrations (0–100 μM) of morelloflavone and measuring the uptake of BrdU by these cells (n = 4). Morelloflavone does not affect the percentage of S-phase cells at a concentration equal to or less than 10μM ($P = 0.079$ by one-way ANOVA on BrdU labelling indices between 0 – 10μM morelloflavone). Morelloflavone, at 100 μM, decreases BrdU labelling indices (****, $P < 0.001$ for BrdU labelling indices between cells treated with 10 and 100 μM morelloflavone). ***(F) MTT (3-[4,5-Dimethylthiazol-2-yl]-2,5-diphenyltetrazolium bromide) VSMC viability assay.*** Morelloflavone is not cytotoxic to VSMCs at concentrations up to 10 μM (*NS* [$P = 0.071$] for MTT survival rate [%] among 0, 0.01, 0.1, 1 and 10 μM, by one-way ANOVA; ****, $P < 0.001$ for MTT survival rate (%) between 10 and 100 μM morelloflavone; n = 4). ***(G) DNA fragmentation assay.*** DNA fragmentation indices decreased as morelloflavone concentrations increased (n = 2 each for 0, 1, 10, and 100 μM; *, $P = 0.032$, by one-way ANOVA). Morelloflavone does not cause apoptosis at concentrations equal to or less than 100 μM.

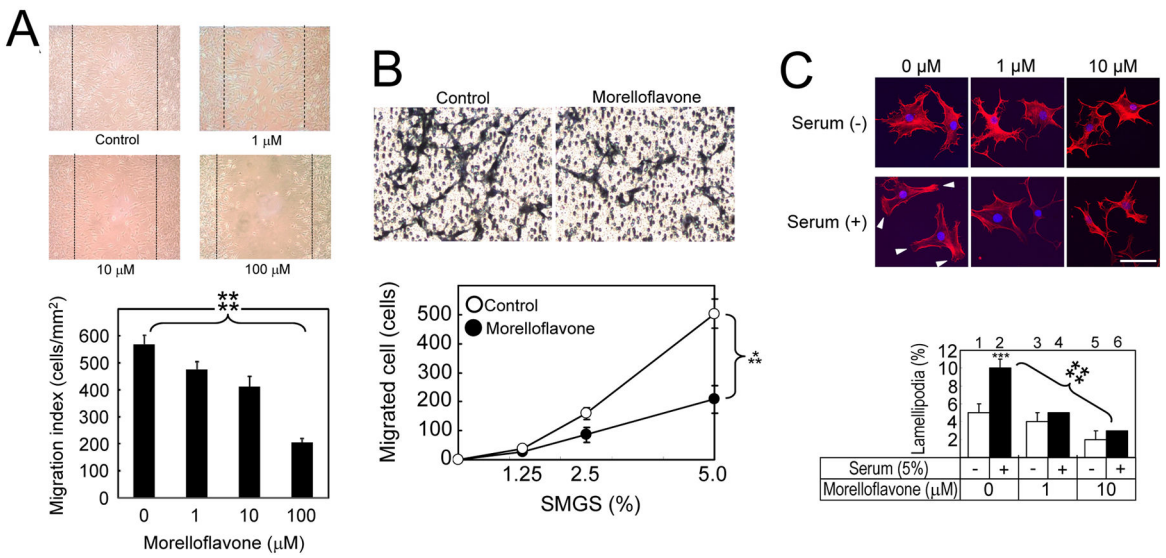


**Fig. 2. Morelloflavone inhibits VSMC migration, invasion and lamellipodium formation**

***(A) Scratch wound cell migration assay.***. Top panels: Photomicrographs of migration patterns of morelloflavone-treated VSMCs. Bottom panel: Migration indices. Migration indices were calculated as migrated cells per unit area (cells/mm$^2$). ****, $P$<0.001 by one-way ANOVA (n = 5). ***(B) Modified Boyden chamber invasion assay.*** Top panels: Photomicrographs of invasion patterns of VSMC in the presence and absence of morelloflavone (1 μM). Bottom panel: The effect of morelloflavone on VSMCs migration. Migrated cell numbers represented the total cell numbers on each test sites (8.0 [mm$^2$]). Morelloflavone at 1μM significantly blocked VSMC migration (***, $P$ = 0.002 by two-way ANOVA, n = 5). SMGS, smooth muscle cell growth supplement (Cascade Biologics, Portland, OR). ***(C) Lamellipodia formation assay.*** Top panels: Confocal microscopy of VSMCs stimulated by sera in the presence of various concentrations of morelloflavone (0–10μM). Arrow, lamellipodia; size bar, 50μm. Bottom panel: Lamellipodium indices calculated as the number of lamellipodia divided by the total number of cells counted. Open bar, no serum; closed bar, 5% serum. Serum stimulation significantly increased lamellipodium indices (***$P$ < 0.005, n = 3) in the absence of morelloflavone. Serum stimulation failed to increase lamellipodium indices in the presence of 1–10 μM morelloflavone. Morelloflavone significantly decreased lamellipodium indices in a concentration-dependent fashion (****, $P$ < 0.001 by one-way ANOVA).

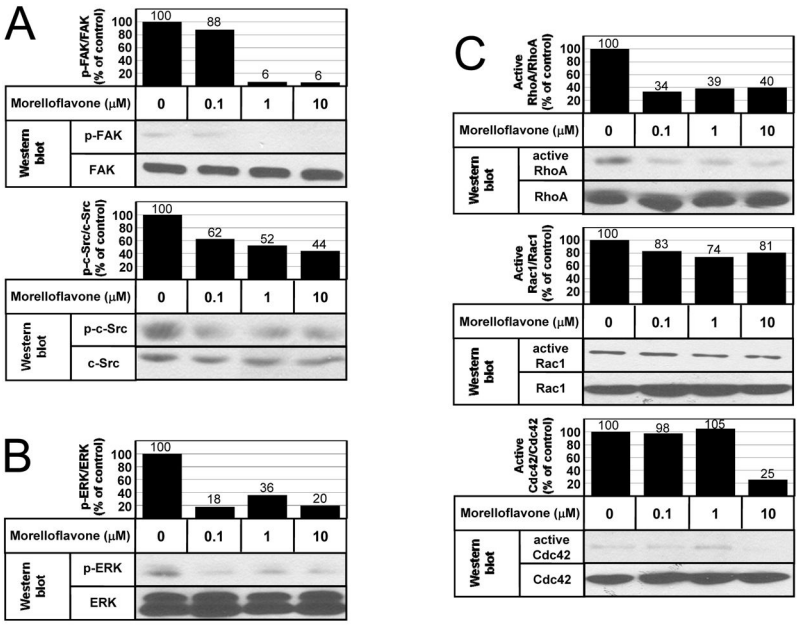


**Fig. 3. Morelloflavone inhibits multiple migration-related kinases**

***(A) Phosphorylation of FAK and c-Src.*** FAK, total focal adhesion kinase; p-FAK, phosphorylated FAK; c-Src, total c-Src; p-c-Src, phosphorylated c-Src. Morelloflavone decreased phosphorylation of FAK and c-Src. The posphorylation indices of a certain kinase (such as p-FAK/FAK) were calculated by dividing the signal intensity of the band of the phosphorylated kinase by the signal intensity of the band of the total kinase, at a given morelloflavone concentration. The indices of untreated cells were normalized to 100. ***(B) Phosphorylation of ERK.*** ERK, total ERK; p-ERK, phosphorylated ERK; Morelloflavone decreased phosphorylation of ERK. ***(C) Activation of RhoA, Rac1, and Cdc42.*** Morelloflavone blocks the activation of RhoA at 0.1 μM, Cdc42 at 10 μM; but it has no significant effect on Rac1 or Cdc42 activation.

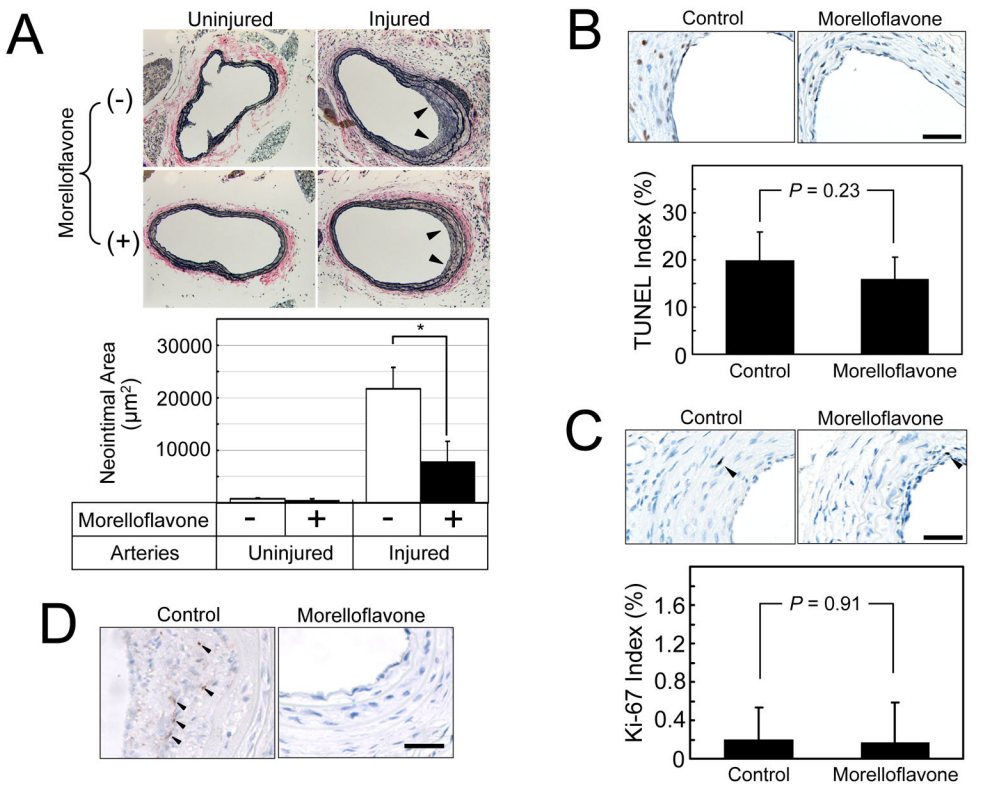


**Fig. 4. Morelloflavone inhibits injury-induced neointimal proliferation in a mouse carotid artery injury model**

***(A) Verhoeff–van Gieson (VVG) staining of mouse carotid arteries***. Upper panel: Photomicrograms of the carotid arteries. Uninjured, right carotid arteries that are sham operated; injured, left carotid arteries in which endothelial cells were denuded by the insertion of an epoxy resin probe; Arrows, neointimal formation. Lower panel: Morphometric analyses of injured and uninjured mouse carotid arteries. *, $P < 0.01$ (Two-sample t-test; n = 9 for control; n = 10 for morelloflavone-treated). Morelloflavone significantly blocked injury-induced neointimal formation in mouse carotid arteries. ***(B) TUNEL apoptosis assays.*** The TUNEL indices were determined as the number of cells with TUNEL-positive nuclei divided by the total number of cells counted and expressed as a percentage (n = 9 for control; n = 10 for morelloflavone-treated). Size bar = 25 μm. ***(C) Ki-67 proliferation assays.*** The Ki-67 indices were determined as the number of cells with Ki-67-positive nuclei divided by the total number of cells counted and expressed as a percentage. Size bar = 25 μm. Oral morelloflavone treatment resulted in reduced neointimal formation, without increasing apoptotic or proliferating cells in the neointima. ***(D) p-ERK staining.*** Phosphorylated ERK was detected by using anti-p-ERK antibody. Size bar = 25 μm. The nuclear p-ERK signals (black arrows) were seen in 42.9 % of the neointima of control animals and in 12.5 % of the neointima of morelloflavone-treated animals (n = 7 and 8, respectively). Oral morelloflavone treatment was associated with reduced p-ERK positivity in the neointima.

## Table

Morphometric Analyses of Uninjured and Injured Carotid Arteries

| Areas (μm$^2$) | Treatment | Uninjured | Injured |
|---|---|---|---|
| Neointimal area | Control | 728.4 ± 796 | 21769.7 ± 11773 |
| | Morelloflavone | 512.0 ± 259 | 7862.7 ± 4047* |
| Medial area | Control | 26492.0 ± 8569 | 43902.7 ± 16916 |
| | Morelloflavone | 30230.6 ± 14393 | 39274.4 ± 15136 |
| Luminal area | Control | 60970.9 ± 4988 | 52743.6 ± 6954 |
| | Morelloflavone | 62340.2 ± 5904 | 62134.5 ± 10740 |
| Internal elastic lamina area | Control | 61699.3 ± 5099 | 74513.3 ± 6320 |
| | Morelloflavone | 62852.4 ± 5900 | 69997.2 ± 11145 |
| External elastic lamina area | Control | 88191.3 ± 6255 | 118415.7 ± 12601 |
| | Morelloflavone | 93083.0 ± 9144 | 102971.6 ± 14326 |

* $P < 0.01$. The neointimal area was calculated as the internal elastic lamina area minus luminal area, while the medial area as the external elastic lamia area minus the internal elastic lamina area.